ELSEVIER

International Journal of Mass Spectrometry 193 (1999) 227–240

International Journal of Mass Spectrometry

Cation–ether complexes in the gas phase: thermodynamic insight into molecular recognition

P.B. Armentrout

Department of Chemistry, University of Utah, Salt Lake City, UT 84112, USA

Received 25 April 1999; accepted 16 July 1999

Abstract

Trends in the bond dissociation energies for the binding of the alkali metal cations, Li^+, Na^+, K^+, Rb^+, and Cs^+, to a series of ethers, 1–4 dimethyl ethers, 1 and 2 dimethoxy ethanes, and the crown ethers, 12c4, 15c5, and 18c6, are discussed. The bond energies have been determined in previous studies by analysis of the thresholds for collision-induced dissociation of the cation–ether complexes by xenon as measured in a guided ion beam tandem mass spectrometer. Details of the analysis of the data are reviewed and the accuracy of the results ascertained by comparison with theoretical results taken from the literature. Combined, the experimental and theoretical results provide an extensive thermochemical database for evaluation of the metal-crown complexes, a simple example of molecular recognition. These results indicate the importance of optimizing the metal–oxygen bond distances and the orientation of the local dipole on the oxygen towards the metal. Further, it is shown that excited state conformers of these complexes are probably observed in several systems as a result of interesting metal-dependent dynamics in the formation of the complexes. (Int J Mass Spectrom 193 (1999) 227–240) © 1999 Elsevier Science B.V.

Keywords: Alkali metal cations; Crown ethers; Bond energies, Collision-induced dissociation

1. Introduction

One of the fundamental components of systems that exhibit molecular recognition is noncovalent interactions [1]. Such interactions involve a subtle interplay of entropic and enthalpic effects that are difficult to separate. Gas phase data on such systems are one means of elucidating these effects and providing fundamental insight into the basis of molecular recognition. One model system that has come under intense scrutiny is the interaction of alkali metal ions with macrocyclic ligands such as crown ethers, c-$(C_2H_4O)_n$ [2–4]. In our work, we have specifically examined the $n = 4$–6 crowns, shown in Fig. 1, which we refer to as 12c4, 15c5, and 18c6, respectively. In a series of related studies [5–10], we have examined the gas-phase thermodynamics of binding between Li^+, Na^+, K^+, Rb^+, and Cs^+ and these crowns as well as related ether complexes, also illustrated in Fig. 1. By using a guided ion beam tandem mass spectrometer, the collision-induced dissociation (CID) of these cation–ether complexes with Xe was examined as a function of collision energy. A rather complicated analysis of these data leads to the binding energies of the alkali metal cation with the ether. These works provide a systematic analysis of

* Corresponding author. E-mail: armentrout@chemistry.chem.utah.edu

PII S1387-3806(99)00165-7

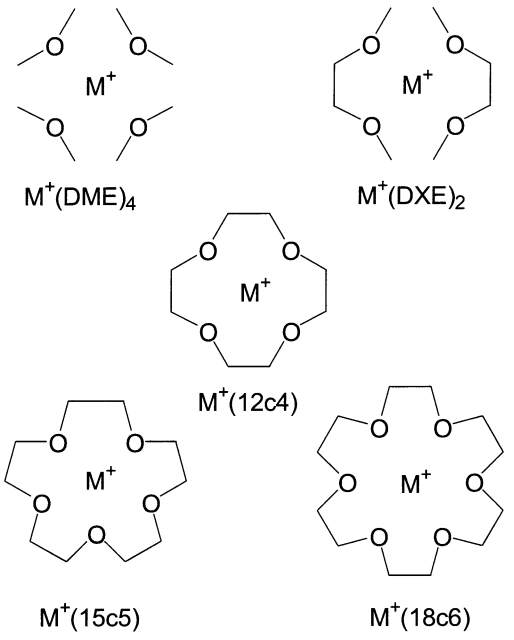

Fig. 1. Schematic geometries of the alkali cation–ether complexes considered in this work. DME = dimethyl ether; DXE = dimethoxy ethane; 12c4 = 12-crown-4, c-$(C_2H_4O)_4$; 15c5 = 15-crown-5, c-$(C_2H_4O)_5$; 18c6 = 18-crown-6, c-$(C_2H_4O)_6$.

the enthalpic contributions to the binding of various alkali ions with ethers, both macrocyclic and cases like the dimethyl ether (DME) molecule where the binding sites are unconstrained by one another (except by steric interactions). In the present work, we correlate all this information for the first time, which provides a clearer view of the trends in the interactions with metal size and with ligand complexity.

It is also useful to realize that this sequence of studies was important in establishing our ability to experimentally measure bond energies to multidentate ligands like the crowns. Previous work [11–16] had established the utility and accuracy of our threshold collision-induced dissociation (TCID) methods for determining metal cation ligand bond energies for monodentate species. Hence, our studies of alkali metal ion binding to 1–4 DME molecules were straightforward. However, the bidentate dimethoxy ethane, $(CH_3OCH_2)_2$ (DXE), and crown ligands presented more of an experimental challenge as these ligands are floppy when uncoordinated but constrained when bound to the metal ion. Further, these complex ligands bind strongly because of their multidentate nature. Both of these circumstances lead to long lifetimes of the collisionally energized complexes such that appearance of dissociation can be shifted to higher collision energies, a so-called "kinetic shift." Comparison of our results for DXE and crown ligands to the sum of the DME ligand bond energies and to theoretical results [5,6,17–20] provides a check on the accuracy of our analysis which includes an estimation of the kinetic shift. These comparisons are discussed further here.

It should also be noted that our studies were motivated by our interest in developing the principals of molecular recognition for use in advanced chemical separations and analytical methodology [21,22]. There is a critical need for such tools in applications such as cleaning up the Hanford nuclear waste site, one of the principal targets of the research conducted at Pacific Northwest National Laboratory. The advancement of separations technology would be greatly enhanced by computational methods capable of accurately predicting host–guest interactions in a variety of condensed phase environments. The experimental results reviewed here act as benchmark data for the development of such theoretical methods.

2. Experimental methods

Details of the experimental methods used to study cation–ether complexes are given in the original works [5–10] so only a brief outline is provided here. A dc discharge in a 10% mixture of Ar in He creates Ar^+ ions that sputter metal ions from either the alkali metal (Li, Na, and K) or metal salt (RbCl and CsCl) contained in a tantalum boat. This takes place at the end of a meter long flow tube [23] where the overall pressure is about 0.5 Torr. Ligand molecules are introduced about 50 cm downstream of the source and attach to the metal ions by three-body condensation. The metal cation complexes are then thermalized by over 10^4 additional collisions with the flow gases before being gently extracted into the rest of the

instrument. After two stages of differential pumping, the ions are passed through a magnetic sector for mass analysis, decelerated to the chosen kinetic energy, and injected into a rf octopole ion beam guide [24]. This device ensures that the ions are not lost even at low kinetic energies or after collision with the neutral reactant. The guide passes through a collision cell (8.24 cm effective length) filled with Xe at a pressure below about 0.2 mTorr. Product ions and remaining reactant ions drift to the end of the octopole where they are extracted and mass analyzed in a quadrupole mass filter. Detection of the ions is achieved using a secondary electron scintillation detector and pulse counting techniques. Data acquisition involves acquiring reactant and product ion intensities as a function of the collision energy both with Xe in the gas cell and with Xe directed to the vacuum chamber. Thus, 50% of all data collection time involves measurement of the background reaction signal. As described elsewhere [25], the raw data, mass-dependent ion intensities versus laboratory ion energies, are converted to reaction cross sections as a function of the center-of-mass energy, the energy available for chemical change.

In order to analyze the kinetic energy dependence and acquire accurate thermochemistry from TCID data, we have previously demonstrated that attention needs to be paid to several things [26]. First, the collision energies must be well defined. In our apparatus, this is achieved by using an octopole ion guide, which perturbs the ion energy distribution much less than a quadrupole guide, and the collision cell is shorter than the octopole such that collisions occur only in the uniform field of the guide. Second, the internal energy of the reactants must be well-characterized. This is achieved by using an atomic neutral reactant and by creating the ions in a flow tube source that thermalizes the ions to a Maxwellian distribution. Third, the collision gas must provide efficient kinetic to internal energy transfer. This dictates the use of Xe, which is heavy and polarizable, while still having no internal modes to carry away energy [26–28]. Fourth, rigorous single collision conditions are required to avoid problems associated with depositing excess (and unknown) energy in secondary collisions. This is achieved by measuring the pressure dependence of the cross sections and extrapolating them to zero pressure [29]. Fifth, the data analysis must include all sources of energy by explicitly considering the full kinetic and internal energy distributions of the reactants. Thus, the data are analyzed by using the following expression:

$$\sigma(E) = \sigma_0 \sum g_i(E + E_i - E_0)^n/E \quad (1)$$

where σ_0 and n are adjustable parameters, E is the relative kinetic energy, and E_0 is the reaction threshold at 0 K. The summation is over the ro-vibrational states of the metal–ligand complex having energies E_i and relative populations g_i, where $\Sigma g_i = 1$. This model is then convoluted with the kinetic energy distributions of the reactants [25].

A particularly important aspect of the data analysis in the crown systems concerns the lifetime of the dissociating ions. In a CID experiment, the ions move through the apparatus in a finite time ($\sim 10^{-4}$ s in our apparatus). Clearly, if the energized complex ions do not dissociate during the flight time between the collision cell and the detector, the dissociation process cannot be observed even if the energized molecule has sufficient energy to dissociate. This decreased probability of observing the true threshold is called a kinetic shift and depends on the complexity of the molecule. We incorporate the Rice-Ramsperger-Kassel-Marcus (RRKM) unimolecular decay theory [30] into our data analysis to estimate the size of this shift [12,31,32]. In our earlier work, we assumed that the transition state was a loose association of the products with reasonable guesses for the vibrational frequencies [5,6,12,31]. During the course of the experiments performed, the sophistication of our analysis improved [32] such that a phase space limit (essentially the loosest transition state possible) was identified as an even more effective means of identifying the molecular parameters of the transition state [7–10]. We verified that this change in the assumption concerning the transition state would not have changed our earlier results within the stated experimental error bars.

Table 1
Bond dissociation energies (in eV) at 0 K of $M^+(L)_x$ for loss of one ligand[a]

	M				
x L	Li	Na	K	Rb	Cs
1 DME	1.71 (0.11)	0.95 (0.05)	0.76 (0.04)	0.64 (0.09)	0.59 (0.05)
2 DME	1.25 (0.06)	0.85 (0.05)	0.71 (0.05)	0.57 (0.05)	0.49 (0.06)
3 DME	0.92 (0.08)	0.72 (0.05)	0.59 (0.04)	*0.38 (0.11)*	0.41 (0.09)
4 DME	0.70 (0.10)	0.63 (0.04)	0.52 (0.08)	0.40 est[b]	0.37 est[b]
1 DXE	2.50 (0.19)	1.64 (0.04)	1.23 (0.04)	0.97 (0.09)	**0.59 (0.05)**
2 DXE	1.44 (0.12)	1.20 (0.08)	0.92 (0.12)	**0.51 (0.12)**	*0.56 (0.07)*
1 12c4	3.85 (0.53)	2.61 (0.13)	1.96 (0.12)	**0.96 (0.13)**	**0.88 (0.09)**
1 15c5		3.05 (0.19)	2.12 (0.15)	**1.18 (0.07)**	**1.04 (0.06)**
1 18c6		3.07 (0.20)	2.43 (0.13)	1.98 (0.13)	1.74 (0.09)

[a] Experimental values taken from [5–10]. Uncertainties in parentheses. Values in bold exceed theoretical values by an average of 73%. Values in italics are about 40% higher than theory.
[b] Estimated value.

Results

3.1. CID cross sections

DME and DXE complexes of the alkali metal ions, $M^+(DME)_x$ and $M^+(DXE)_y$, all dissociate by sequential loss of intact ligands upon collisional activation [5–9]. This is illustrated by the data shown for $Na^+(DME)_4$ in Fig. 2, which is typical of these complexes for all metal cations. Analysis of the primary thresholds (loss of a single ligand) for the DME complexes where $x = 1$–4 and the DXE complexes for $y = 1$ and 2 yields the 0 K bond energies listed in Table 1. The reproduction of the data as shown in Fig. 2 is typical. It can be seen that there is a considerable difference between the data (and the full line modeling it) and the dashed line, which represents the cross section in the absence of the internal and translational energy distributions of the reactants. Clearly, these distributions have a significant effect on the thermochemistry obtained and must be included in the data analysis to derive meaningful results. Note that in these cases, the real threshold, E_0, lies at an energy *above* the energy where the cross section rises from zero.

Results for the crown ethers are also qualitatively similar to the smaller systems although the thresholds are now substantially higher, partly because of the multidentate character of these ligands. In all cases, loss of the intact crown ether is the dominant dissociation product [6–10]. Li^+(12c4) also exhibits substantial fragmentation of the ring [6], whereas none of the other M^+ (crown) complexes exhibit such behav-

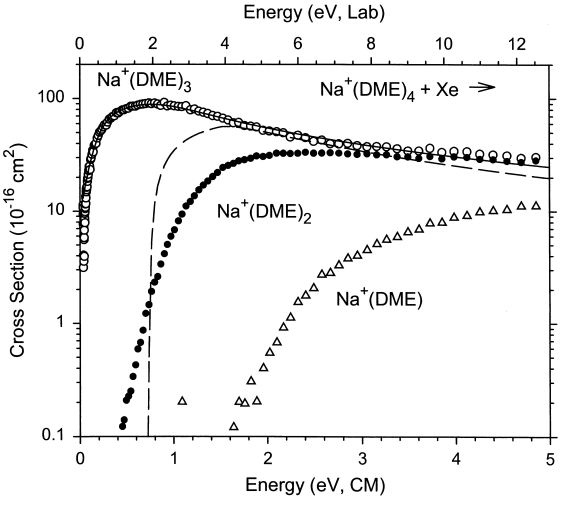

Fig. 2. Cross sections for collision induced dissociation of $Na^+(DME)_4$ with Xe as a function of kinetic energy in the center-of-mass frame (lower *x* axis) and laboratory frame (upper *x* axis). The dashed line shows the model of eq. 1 for reactants with no internal energy and includes a model for subsequent dissociation of the primary product at higher energies. The full line is this model convoluted with the internal and kinetic energy distributions of the reactants.

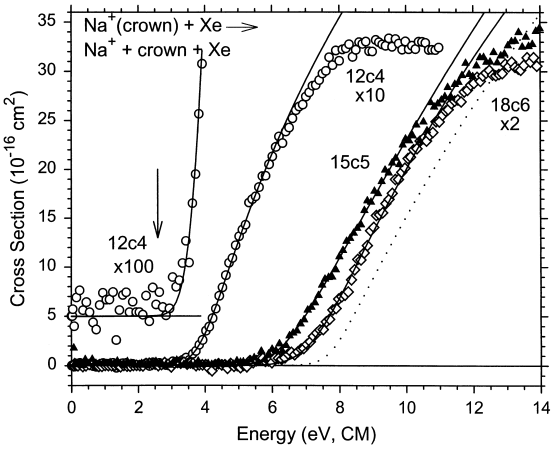

Fig. 3. Cross sections for collision induced dissociation of Na^+(12c4) (open circle, multiplied by a factor of 10), Na^+(15c5) (closed triangle), and Na^+(18c6) (open diamond, multiplied by a factor of 2) with Xe as a function of kinetic energy in the center-of-mass frame. Data for Na^+(12c4) is also shown expanded by a factor of 100 and offset from zero. The dotted line shows the model of Eq. (1) for the Na^+(18c6) reactants with no internal energy. The solid lines are this model and comparable ones for Na^+(12c4) and Na^+(15c5) convoluted with the internal and kinetic energy distributions of the reactants.

ior. [Unfortunately, data for Li^+(15c5) and Li^+(18c6) could not be obtained because of limitations in our mass spectrometer associated with simultaneous handling of the very heavy reactant ion and the very light Li^+ product ion.] Results for the complexes of Na^+ with three crown ethers are shown in Fig. 3. Good reproduction of the data using the model discussed above is obtained as shown for all three complexes.

The key question in the analysis of the data for the crowns is whether the kinetic shifts are properly calculated. The extent of this issue is illustrated in Fig. 3. The arrow shows the E_0 threshold derived for the 12c4 complex (Table 1). This value agrees reasonably well with the energy where the cross section first deviates from zero but only once the data are expanded considerably. On the full scale part of the diagram, the apparent threshold is almost 1 eV higher than the threshold derived from analysis. The shifts are more dramatic in the 15c5 and 18c6 data which both have derived thresholds near 3 eV (Table 1), while the apparent thresholds are much higher and different from one another, about 4.5 and 6 eV, respectively. In these cases, expansion of the data moves the thresholds down considerably from these values but the dynamic range of our experiment is insufficient to directly observe the true threshold. Clearly, the analysis involves an extensive extrapolation of the data and requires that the collisional excitation of the complex and the subsequent unimolecular dissociation be treated correctly.

3.2. Overall accuracy of the bond energies

In assessing the trends in the thermochemistry as the complexity of the ligands and the metal varies, it is important to have confidence in the accuracy of the experimental numbers. As noted above, a wide variety of systems involving monodentate ligands have previously been studied using the experimental TCID methods outlined above and these have proven to yield accurate thermochemistry where literature information is available for comparison [11–16]. For the multidentate ligands, the present work comprises the first comprehensive test of TCID methods. As noted above, one test of the accuracy of the bond energies for multidentate ligands is whether there is reasonable agreement with the sums of the bond energies for the $M^+(DME)_x$ complexes having the same number of oxygen sites. As we shall see, these comparisons generally yield a reasonable agreement; however, this test is not definitive as we do not expect these numbers to be exactly the same. Indeed, the differences between them provide useful information if they are accurate. Hence a comparison with theory provides a better overall test.

Fortunately, good ab initio calculations on all these systems have been performed by Feller and coworkers [5,6,17–20] in collaboration with our experimental studies. Although higher level calculations were performed for some complexes, all complexes considered here were calculated at a uniform level of theory that involves geometry optimizations at the RHF/6-31+G* level followed by single point energy calculations at the MP2/6-31+G* level. Generally, diffuse functions were not included on all atoms and effective core potentials were used for K, Rb, and Cs where the valence and $(n - 1)$ atomic shells were

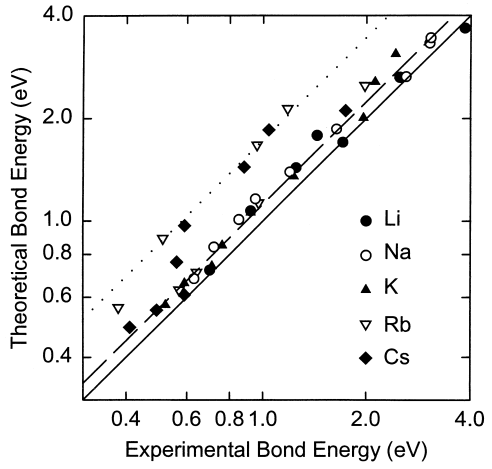

Fig. 4. Theoretical bond energies for the $M^+(DME)_x$ (x = 1–4), $M^+(DXE)_y$ (y = 1–2), and M^+(crown) (crown = 12c4, 15c5, and 18c6) vs. experimental bond energies for these complexes where M = Li (closed circle), Na (open circle), K (closed triangle), Rb (open inverted triangle), and Cs (closed diamond). Experimental values are taken from Table 1 and theoretical values are from [17–20]. Note that both scales are logarithmic.

excluded from the core definition. The final values are also corrected for basis set superposition errors using the counterpoise correction of Boys and Bernardi [33].

A comparison of our experimental values with these theoretical values for all systems listed in Table 1 is shown in Fig. 4. Note that this plot covers an order of magnitude in bond energies. It can be seen that except for several values involving Rb and Cs, the agreement is very good. Indeed, for all complexes involving Li, Na, and K (25 values), we find that theory is uniformly 12 ± 8% higher than experiment (see dashed line in Fig. 4). If the DME and 18c6 complexes of Rb and Cs are included [another 8 values excluding Rb^+ $(DME)_3$], then the discrepancy remains 12 ± 8%. There are some indications that more extensive basis sets will reduce this difference [5] although this conclusion is not uniform in all systems [17,18]. Nevertheless, this comparison demonstrates that the experimental bond energies are accurate within their stated uncertainties and that the trends among most of the bond energies are reasonable.

This conclusion is particularly important for the crown ether complexes because of the difficulty associated with the kinetic shift analysis, as noted above. We note with some satisfaction that the theoretical bond energies for Na^+(15c5) and Na^+(18c6) are similar, 3.3 and 3.4 eV, respectively, in good agreement with the relative threshold values in Table 1 but in contrast to the apparent thresholds shown in Fig. 3. One can wonder whether the experimental values are lower than theory because the kinetic shift has been improperly estimated. There are two arguments against this, however. First, the 12% discrepancy between experiment and theory is observed for the DME complexes where the kinetic shifts are small or nonexistent (except for the Li complexes where they vary between 0.0 and 0.3 eV). Second, to make the experimental values agree better with theory, the thresholds would have to be higher and the kinetic shifts smaller. This requires that we assume a transition state for dissociation that is looser than the one used in our analysis; however, the values listed in Table 1 utilize a transition state that is already the loosest we can reasonably imagine.

The conclusion that the agreement between the experimental and theoretical bond energies is reasonable is clearly inappropriate for six values. These include the 12c4 and 15c5 complexes of Rb and Cs along with $Rb^+(DXE)_2$ and $Cs^+(DXE)$ and are marked in bold in Table 1. These values show serious but uniform disagreements such that the theoretical values lie systematically above experiment by 73 ± 7% (see dotted line in Fig. 4). These discrepancies are presumed to have an experimental origin, which we discuss in detail in sec. 4, as it is difficult to understand why theory would be systematically off in these particular cases and there are other indications that the experimental values in these cases are low.

Finally, there are two additional values, for $Rb^+(DME)_3$ and $Cs^+(DXE)_2$, that have discrepancies between experiment and theory of about 40%. In both cases, these differences are within the combined experimental and theoretical errors, such that the discrepancy is not severe. However, we think it likely that the true value for $Rb^+(DME)_3$ is closer to the upper limit of our experimental range. The situation is less clear for $Cs^+(DXE)_2$, as is discussed in Sec. 4.

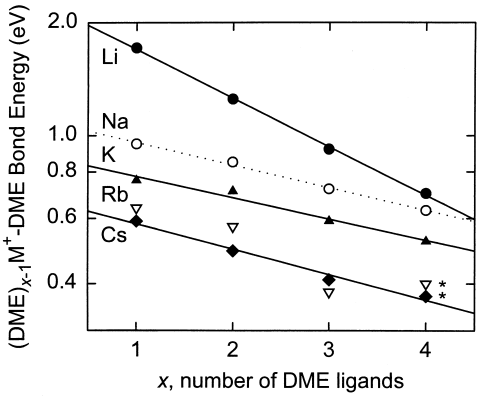

Fig. 5. Sequential bond energies for $M^+(DME)_x$ complexes as a function of the number of dimethyl ether ligands. Experimental values are shown for M = Li (closed circle), Na (open circle), K (closed triangle), Rb (open inverted triangle), and Cs (closed diamond). Starred points are estimated. Note that the energy scale is logarithmic.

4. Discussion

4.1. Dimethyl ether complexes

The experimental bond energies obtained for all five metal cations are plotted in Fig. 5. It can be seen that the bond energies fall in the order Li > Na > K > Rb > Cs. This is expected for electrostatic interactions because the smaller the ion is, the closer the metal–ligand bond distance (see Table 2) and the stronger the electrostatic interaction. It can also be seen that the bond energies gradually decrease as the number of ligands around the metal ion increases. This is also typical behavior for electrostatic interactions. The bond energies decrease because of electron delocalization to the metal center and because of ligand–ligand repulsion. (See the Natural Energy Decomposition Analysis of $Li^+(DME)_x$ complexes in [5]). These effects are also illustrated by the gradually increasing bond lengths with *x*, Table 2.

More subtle effects are also shown by these results. Note that the decrease in bond energies with increasing ligation is more rapid for Li than for the other metals. Clearly, this can be rationalized by more severe ligand–ligand repulsions around the smaller cation. Indeed the trends for Na, K, Rb, and Cs are very similar, indicating that there is much less ligand–ligand interaction in these systems. Note that the calculated M–O bond lengths mirror this conclusion: for Li, the bond length increases by 10% in going from $x = 1$ to 4, whereas for the other metals, the increase is between 3% and 5%. The patterns in the bond energies also suggest that the best $Rb^+(DME)_3$ bond energy may be slightly higher than the mean value measured, probably toward the upper limit of the experimental uncertainty. This conclusion agrees with that independently drawn by comparison with theory (as discussed in Sec. 3).

As expected, calculations indicate that the DME ligands bind to the metal cations by pointing the oxygen atom toward the metal ion [5,17]. Thus, the dipole moment of DME is aligned in the most favorable orientation. As ligands are added to the complex, the ground state structures are generally consistent with minimizing ligand–ligand repulsions. Hence, the oxygens array themselves around the metal ion in linear (∠OMO = 180°), trigonal planar (∠OMO = 120°), and tetrahedral (∠OMO = 110°) arrangements for the $x = 2$–4 complexes, respectively [5,17]. The only exceptions are the $M^+(DME)_2$ complexes for M = K, Rb, and Cs where the complexes adopt bent geometries, a result attributed to metal core polarization [17,34]. However, these bent geometries are favored by less than 0.06 eV compared to linear geometries, and the OMO bond angle depends critically on the level of theory [17], as shown in Table 2.

4.2. Dimethoxyethane complexes

As for the DME complexes, the bond energies to DXE decrease as the metal gets larger and with increasing ligation. It can also be seen that the DXE bond energies exceed those for a single DME ligand for all metals but Cs and the second DXE bond energy exceeds the third DME bond energy for all metals, as expected for bidentate versus monodentate ligands. A more insightful way of comparing this thermochemistry is to evaluate complexes having the same number of oxygens, the binding sites in both ligands. This kind of comparison is found in Table 3 where the sum

Table 2
Metal–oxygen bond lengths (in angstrom) and O–M–O bond angles for $M^+(L)_x$ complexes[a]

	M				
x L	Li	Na	K	Rb	Cs
1 DME	1.81	2.20	2.64	2.89	3.12
2 DME	1.85	2.23	2.68	2.92	3.16
	180°	180°	133° (89°)[b]	126° (81°)[b]	114° (75°)[b]
3 DME	1.90	2.27	2.71	2.95	3.20
	120°	120°	120°	120°	120°
4 DME	1.99	2.32	2.75	2.98	3.22
	110°	110°	110°	110°	110°
1 DXE	1.86	2.25	2.68	2.92	3.16
	90°	76°	63°	58°	54°
2 DXE	1.96	2.31	2.75	2.99	3.23
	84°	73°	62°	57°	52°
12c4	2.00	2.34	2.76	2.99	3.22
	83°	72°	61°	56°	52°
18c6 (sym)	2.20 (S_6)	2.48 (C_1)	2.81 (D_{3d})	2.98 (C_{3v})	3.22 (C_{3v})

[a] All values are from RHF/6-31+G* calculations except as noted. Values for lithium complexes are taken from [5] and [6]. All other results for DME complexes are from [17]. All other values for DXE and 12c4 are from [18]. Values for 18c6 are from [19].
[b] MP2/6-31+G* optimized geometries.

of the bond energies in $M^+(DME)_2$ is compared to $M^+(DXE)$ and the sum of the third and fourth bond energies in $M^+(DME)_4$ is compared to the $(DXE)M^+$–DXE bond energy. Clearly the DXE bond energies are similar to the sums of the DME bond energies but are consistently lower by about 10%–20% (except for the Cs complexes). This is also shown in Fig. 6. This difference can be rationalized on the basis that the C–C bond along the DXE backbone constrains the orientation of the oxygens toward the metal ion. In essence, the local dipoles in DXE cannot simultaneously orient themselves toward the metal ion and maintain the optimal M–O bond distance because of the restriction in geometry. The DME ligands are not constrained and can optimize both the orientation and M–O bond distance.

Table 3
Comparison of bond energy sums for $M^+(DME)_x$ complexes with bond energies for complexes with multidentate ligands[a]

	M				
x L	Li	Na	K	Rb	Cs
			Systems with two oxygens		
1 + 2 DME	2.96	1.80	1.47	1.21	1.08
DXE	2.50/84%	1.64/91%	1.23/84%	0.97/80%	**0.59/55%**
3 + 4 DME	1.62	1.35	1.11	0.89[b]	0.78
2 DXE	1.44/89%	1.20/89%	0.92/83%	**0.51/57%**	*0.56/72%*
			Systems with four or more oxygens		
1 − 4 DME	4.58	3.15	2.58	1.99	1.86
1 + 2 DXE	3.94/86%	2.84/90%	2.15/83%	**1.48/74%**	***1.15/62%***
12c4	3.85/84%	2.61/83%	1.96/76%	**0.96/48%**	**0.88/47%**
15c5		3.05/97%	2.12/82%	**1.18/59%**	**1.04/56%**
18c6		3.07/97%	2.43/94%	1.98/99%	1.74/94%

[a] Values in bold and italic are derived from values so identified in Table 1.
[b] This value is calculated using the upper limit of our experimental value for the $(DME)_2Rb^+$–DME bond energy, see text.

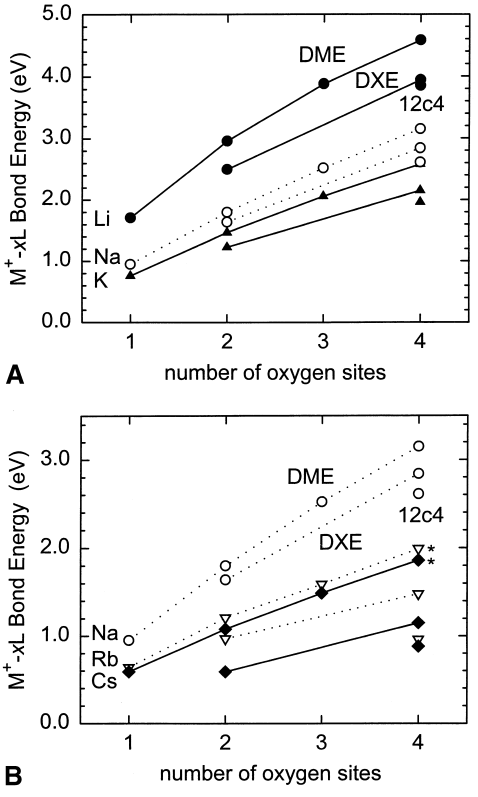

Fig. 6. Total experimental bond energies for dissociation of $M^+(L)_x$ complexes to $M^+ + x$ L as a function of the total number of oxygens in the ligands. Part a shows values for M = Li (closed circle), Na (open circle), K (closed triangle), while part b gives values for Na (open circle), Rb (open inverted triangle), and Cs (closed diamond). Starred points are estimated. These groupings are chosen for clarity. The upper points and line for all metals show results for L = DME and x = 1–4, the lower points and line show results for L = DXE and x = 1 and 2, and the remaining point gives the bond energy for 12c4.

Calculated geometries of these complexes involve binding both oxygen atoms to the metal cation center [6,18]. The OCCO dihedral angle changes from 74° in the free DXE ligand (having a gauche orientation about the C–C bond) to 48°, 55°, 59°, 61°, and 63° in the Li–Cs complexes, respectively. Similar dihedral angles are obtained for the $M^+(DXE)_2$ complexes where the two ligands lie perpendicular to one another on either side of the metal ion. As shown in Table 2, the calculations find that the M–O bond lengths in $M^+(DXE)$ are nearly the same as for the $M^+(DME)_2$ complex, whereas those for $M^+(DXE)_2$ are comparable to those for $M^+(DME)_4$. However, the OMO bond angles are much smaller in the DXE complexes than in the comparable DME complexes. In essence, this shows that the decrease in the bonding can largely be attributed to the inability of the local dipoles at the oxygen centers to align with the metal ion, rather than the failure to optimize the M–O bond distance.

In the case of the Cs complexes and $Rb^+(DXE)_2$, the DXE bond energies are about half as strong as the sum of the DME bond energies (Table 3). Note that these are the same systems identified as disagreeing with theory. Apparently, the experimental threshold being measured does not correspond to the ground state of the DXE complexes in which both oxygens are bound to the metal ion. Rather, it appears that we have measured the bond energy of an excited conformer that has only a single M^+–O bond. This is suggested by the observation that these DXE bond energies are comparable to the analogous DME bond energies, e.g. the Cs^+–DXE bond energy is approximately the same as the Cs^+–DME bond energy, etc. This is experimentally plausible as long as an appreciable amount of such an excited conformer is present in our reactant ion beam. In such circumstances, our threshold measurements are sensitive only to the lowest energy dissociation pathway and the observation of a secondary threshold (attributable to the ground state conformer) is difficult to observe because of the extensive broadening and averaging over reactant energy distributions and dissociation lifetimes.

We speculate that such high energy conformers are produced for some metals in the following way. DXE has two low-lying conformations in the gas-phase, the gauche conformation (or tgt, trans–gauche–trans) geometry that associates both oxygen atoms to the metal ion and the trans conformation (or ttt, trans–trans–trans) geometry in which the central C–C bond has the two methoxy groups trans to one another. This latter geometry is calculated to lie slightly lower in energy than the tgt conformation [6,18]. Experimentally, the metal complexes are generated by association of the metal ion with the free ligand, followed by thermalization to remove the energy released in forming the metal–ligand bond. Clearly the ground state conformation of the DXE complexes can be formed by

association of M^+ with the gauche conformer, but association of the trans conformer with M^+ can form an excited conformation of the complex. Apparently, for most metals, such an excited conformation has sufficient internal energy that it can rearrange to the ground state conformation before being completely thermalized. The barrier for this rearrangement is associated with rotation around the C–C bond and should be larger for the metal cationized complexes than the free ligand because hydrogen atoms on the rotating carbon have to pass the metal cation. One can imagine that this rearrangement is driven electrostatically and is sterically hindered more by larger cations. Thus, it seems reasonable that the barrier varies with the metal cation. For the Cs complexes, it appears that a significant number of these excited conformers get trapped. We attribute this to a smaller electrostatic driving force because the charge is more diffuse on the large Cs ion and a larger steric hindrance to rotation. Likewise, excited conformers appear to occur for $Rb^+(DXE)_2$ but not $Rb^+(DXE)$. This is presumably because the first ligand reduces the effective charge on the metal cation and may also contribute steric inhibition to the rearrangement to the ground state conformer.

4.3. 12-Crown-4 complexes

As for the simpler ligands, the bond energies for 12c4 decline as the metal ions get larger. A comparison of the 12c4 bond energies with the sum of the bond energies for the $M^+(DME)_4$ complex (Table 3) shows that the crown bond energies are about 80% of the unconstrained DME complex for M = Li, Na, and K. Further, the bond energies to 12c4 lie slightly below the sum of the bond energies in $M^+(DXE)_2$ [Fig. 6(a)]. This seems reasonable as the C–C bond backbone of the crown prevents a simultaneous optimization of the M–O bond length and the orientation of the oxygen dipole towards the metal ion. This constraint is more severe for 12c4 than two DXE ligands because of the additional C–C bonds. As the M–O bond lengths of the $M^+(12c4)$ complexes are nearly the same as for the $M^+(DME)_4$ complexes (Table 2), we again attribute the decline in bond energies to the inability of the local dipole to align in the most optimum orientation in the crown complexes.

In contrast to the Li, Na, and K complexes of 12c4, the Rb and Cs complexes have bond energies that are only half of the analogous $M^+(DME)_4$ bond energy sum [Table 3 and Fig. 6(b)]. These same complexes were identified as being anomalously low by comparison with theory (Table 1). Note that the $Rb^+(12c4)$ bond energy is comparable to the $Rb^+(DXE)$ bond energy, and that both 12c4 complexes have bond energies that are about 80% of the sum of the bond energies in $M^+(DME)_2$. In analogy with our discussion of the anomalous DXE complexes of Rb and Cs, this suggests that the experimental bond energies refer to an excited conformation where only two of the oxygens in 12c4 are involved in the bonding.

On the basis of this hypothesis, Hill et al. [18] looked for and found such a conformation computationally. For all metal cations, the ground state conformation of the $M^+(12c4)$ complexes has C_4 symmetry such that all four oxygens point towards the metal ion, which sits above the plane of the crown ether by a height that depends on the metal ion radius. This is indicated by the OMO bond angle given in Table 2. The excited state conformation identified has C_{2v} symmetry in which two oxygens (opposite one another on the ring) point towards the metal ion and the other two point away, consistent with the relative bond energies noted previously. Indeed, the calculated bond energies for these conformers are 1.08 and 0.95 eV for Rb and Cs [18], respectively, compared to our measured values of 0.96 and 0.88 eV (Table 1). Note that the discrepancies between these values are 12% and 8%, respectively, the same difference between experiment and theory observed for most other metal cation–ether complexes (see above).

A key observation in understanding why such excited conformations are observed is that the ligand geometry is similar to the ground state conformation of the free 12c4 ligand, which has S_4 symmetry. As for the DXE complexes of Rb and Cs, it appears as though the production of excited conformers of $Rb^+(12c4)$ and $Cs^+(12c4)$ are kinetically favored because the free ligand (having S_4 symmetry) attaches

to the metal cation and then is thermalized in our ion source. Presumably, a mixture of this excited conformer and the ground state conformer are formed, but our experiment is sensitive primarily to the conformer having the lowest energy dissociation channel. Hill et al. [18] also identified such an excited state in the case of K^+(12c4) whereas experimentally there is no indication for the presence of such a conformer. We have proposed [9] that this is because the barrier between the ground and excited state conformations depends on the metal. Again, a smaller metal may be capable of electrostatically driving the rearrangement and a larger metal may sterically hinder the rearrangement. Hill et al. [18] crudely estimated the barrier between the conformers using a linear synchronous transit (LST) method and found it to be about 0.5 eV, independent of metal identity for K, Rb, and Cs. They also noted that the rearrangement probably occurs stepwise as they could identify another excited conformation having C_1 symmetry in which three of the oxygens point toward the metal and the fourth points away. It is possible that this LST pathway is not representative of the lowest energy path for rearrangement. Indeed, it is interesting to note that in the C_{2v} geometry of K^+(12c4), all four M–O bond distances are comparable to each other (2.751 and 2.757 Å) and to the M–O bond lengths in the ground state C_4 conformation (2.757 Å) [18]. For the Rb and Cs complexes, the M–O bond lengths in the C_{2v} geometry differ much more (by 0.053 and 0.106 Å, respectively) and all are slightly longer than in the ground state C_4 conformation. Because K^+ lies so close to the "nonbonding" oxygens in the excited C_{2v} conformation, it seems plausible that there is a stronger electrostatic driving force for the rearrangement to the ground state than in the Rb and Cs systems.

4.4. 15-Crown-5 complexes

The bond energies to 15c5 exceed those to 12c4 for all metals studied (by an average of 17 ± 6%). This seems reasonable given the increase in the number of oxygen binding sites, although clearly the increase is not 25% as might be expected on the basis of the numbers of oxygens. Again this can be attributed to geometric constraints imposed by the crown backbone. As for the 12c4 complexes, the bond energies for the alkali metal cations complexed with 15c5 have similar values to the sum of the bond energies in $M^+(DME)_4$ for the lighter cations, Na and K, while those for Rb and Cs are much smaller (Table 3). Again these latter two complexes have bond energies that disagree with theory (Table 1). We attribute these low bond energies to excited state conformations whose formation is kinetically favored and rearrangement barriers to the ground state conformations that depend on the metal.

4.5. 18-Crown-6 complexes

In contrast with the smaller crowns, the strength of the 18c6 crown ether bonds to all the alkali metal cations (Na^+–Cs^+) is comparable to the sum of the bond energies for $M^+(DME)_4$ (Table 3). Further, these values are in reasonable agreement with theory [19] and the trends among the metals agree nicely. The 18c6 bond energies are much less than 50% greater than the 12c4 bond energies, as might have been predicted on the basis of the increase in the number of oxygen centers available for bonding. For the larger metal ions (K^+, Rb^+, and Cs^+), theory finds that the M–O bond lengths for the 18c6 complexes are comparable to those for $M^+(DME)_4$ (Table 2). Thus, the smaller than expected binding for 18c6 can be attributed to the constraints on the metal–oxygen orientation imposed by the crown backbone. In contrast, the smallest cations, Li^+ and Na^+, have larger M–O bond lengths in the 18c6 complexes than in $M^+(DME)_4$ (Table 2), such that a smaller electrostatic interaction should occur for the multidentate crown complex than for the independent DME ligands.

One interesting aspect of these results is that there is no indication of excited conformers for the Rb^+ and Cs^+ complexes, in contrast to the cases of 12c4 and 15c5 bound to these metal cations. The ground states of these two complexes have C_{3v} symmetry in which three alternating oxygens point towards the metal ion which sits above the plane of the crown ring whereas the other three oxygens point away from the metal ion (although the difference in M–O bond distances is

fairly small, 0.004 and 0.008 Å, respectively). As this conformation is similar to the ground state conformation of the free 18c6 ligand, the kinetically favored conformation of the M^+(18c6) complexes likely to be formed in our flow tube source is the ground state conformation, in contrast to the situation for the smaller crowns.

Finally, we note that our experimental bond energies for K^+(18c6) and Cs^+(18c6) are much larger than values extracted from collision-induced dissociation experiments performed in an ion cyclotron resonance mass spectrometer [35], 1.73 and 1.39 ± 0.35 eV, respectively. The detailed explanation for the large discrepancy between these experiments is unclear, but the analysis of these experiments did not address many of the issues (described above) that are needed to extract accurate thermochemistry from CID experiments.

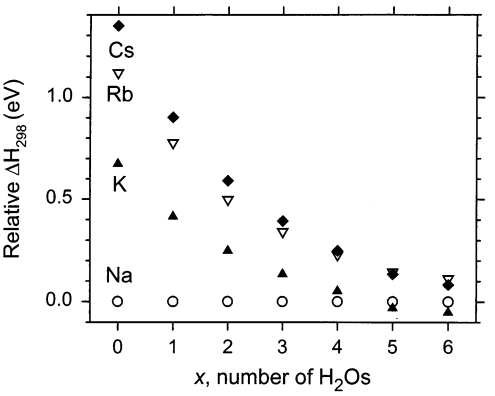

Fig. 7. Experimental enthalpy at 298 K of reaction (2) for M = K (closed triangle), Rb (open inverted triangle), and Cs (closed diamond) relative to that for Na (open circle) as a function of *x*, the number of water molecules originally solvating the metal ion.

4.6. Selectivity of 18-crown-6 for alkali metal cations in aqueous solution

The crown ethers have provoked much attention because 18c6 binds K^+ selectively over Rb^+, Cs^+, and Na^+ (in that order) in an aqueous environment [36]. In contrast, the gas-phase bond energies determined here for the various alkali metal cations with 18c6 clearly indicate that Na^+ is most strongly bound, by a considerable margin. It has been shown [10,19] that this can be understood by considering the competition between solvation of the cations by water and complexation by the crown,

$$M^+(H_2O)_x + 18c6 \rightarrow M^+(18c6) + x\ H_2O \qquad (2)$$

Fig. 7 shows the relative enthalpy for this reaction at 298 K given gas-phase hydration enthalpies taken from the literature [37,38]. As the entropies of reaction should be similar for all metals, this plot is also a fair representation of the relative free energies for this reaction. It can be seen that differences among the various cations drop dramatically as the number of waters increases, because the smaller cations bind both 18c6 and water more effectively. Fig. 7 shows that complexation of Na^+ by 18c6 is favored until the number of water molecules that have to be displaced nears a complete solvent shell. At this point, K^+ is selectively bound by the crown, in agreement with the findings in solution. It is interesting to note that for all metal cations, reaction (2) is endothermic for $x = 6$ but exoergic because entropy strongly favors the forward reaction. In essence, this is one demonstration that the origin of the macrocyclic effect is largely an entropic one.

It should also be noted that Fig. 7 does not reach the point where Na^+ is the least favored alkali, as observed in solution. We have hypothesized [10] that this is because of differential effects regarding the hydration of the M^+(18c6) complex, an effect that has been considered theoretically by Feller [39]. In the 18c6 complexes of K, Rb, and Cs, the metal is exposed and can be directly solvated, while the 18c6 crown surrounds the smaller Na^+ cation, shielding it from being solvated directly. This should stabilize the larger metal ion crown complexes relative to Na^+(18c6). Overall, this comparison demonstrates that the selective binding of K^+ by 18c6 in aqueous media is a delicate balance of solvation versus complexation enthalpy, entropic effects, and the solvation of the resultant complex. Clearly, these factors depend critically on the identity of the solvent.

5. Conclusions

Kinetic energy dependent collision-induced dissociation in a guided ion beam tandem mass spectrometer has been used to determine the absolute bond dissociation energies of Li^+, Na^+, K^+, Rb^+, and Cs^+ with several simple and complex ethers [5–10]. The ligands include 1–4 monodentate dimethyl ethers (DME), 1 and 2 bidentate dimethoxy ethanes (DXE), and the multidentate crown ethers, 12c4, 15c5, and 18c6. To obtain accurate thermochemistry, the analysis of these results must include consideration of the effects of multiple collisions, internal and translational energy distributions of the reactants, and the dissociation lifetimes of the energized complexes. As reviewed here, we find that most of these experimental results agree nicely with ab initio calculations of Feller and coworkers [5,6,17–20] with a systematic difference such that the theory is 12 ± 8% higher. This confirms the utility of the experimental method for multidentate ligands.

Larger differences between experiment and theory (about 73%) are obtained for several complexes with Rb^+ and Cs^+, specifically those involving DXE, 12c4, and 15c5, but not 18c6. This is explained by the presence of less strongly bound conformers that are formed in kinetically favored processes in the experimental ion source. Several arguments support the plausibility of this assignment. In future work, we hope to test this hypothesis using electrospray ionization in which these complexes are generated by extracting them directly from equilibrated structures in solution. It might also be possible to observe the consequences of such excited state conformers in the formation of such complexes by radiative association.

Overall, the bond energies determined in these studies demonstrate that the bonding is dominated by electrostatic interactions and the strength of the interaction changes inversely with the size of the metal ion, i.e. they scale with charge density. Detailed comparisons of the bond energies for the DME complexes, where the ligands are unconstrained, with those for the multidentate DXE and crown ligands show that the former bond more strongly in all cases. This is attributed to geometric constraints introduced by the C–C backbone in the multidentate ligands. Theoretical calculations demonstrate that metal–oxygen bond lengths in complexes having the same number of donor oxygen atoms are similar in all cases [5,6,17–20]. Thus, the decrease in bonding can be assigned largely to imprecise alignment of the local dipole on the oxygen atoms (the C–O–C subunit) towards the metal cation. The fact that both the alignment and M–O bond lengths are critical factors in determining the strength of the cation–ether bonds agrees with the conclusions of Hay and co-workers on the basis of molecular mechanics and ab initio calculations [40,41].

Finally, by combining the gas-phase bond energies of the alkali metal cations to 18c6 and the sequential hydration energies of these cations, insight into the selectivity of the crowns for metal ions is obtained. This shows that such selectivity is *not* simply an intrinsic property of the metal cation–crown complex, but depends critically on solvation phenomena. This indicates that an accurate determination of molecular recognition in such systems needs to include the media in some detail.

Acknowledgements

The author is particularly grateful to his experimental co-workers, Michelle B. More, and Doug Ray, for their participation in these studies. Theoretical colleagues, Dave Feller, Eric Glendening, and Susan Hill, also made this project rewarding. Funding for this work was provided by the National Science Foundation and the Division of Chemical Sciences, Office of Basic Energy Sciences, U. S. Department of Energy.

References

[1] Principles of Molecular Recognition, A.D. Buckingham, A.C. Legon, and S.M. Roberts (Eds.), Blackie Academic, Glasglow, 1993.
[2] F. DeJong, D.N. Reinhoudt, Adv. Phys. Org. Chem. 17 (1990) 279, and references therein.

[3] R.M. Izatt, J.S. Bradshaw, S.A. Nielsen, J.D. Lamb, J.J. Christensen, D. Sen, Chem. Rev. 85 (1985) 271.
[4] R.M. Izatt, K. Pawlak, J.S. Bradshaw, R.L. Bruening, Chem. Rev. 91 (1991) 1721.
[5] M.B. More, E.D. Glendening, D. Ray, D. Feller, P.B. Armentrout, J. Phys. Chem. 100 (1996) 1605.
[6] D. Ray, D. Feller, M.B. More, E.D. Glendening, P.B. Armentrout, J. Phys. Chem. 100 (1996) 16116.
[7] M.B. More, D. Ray, P.B. Armentrout, J. Phys. Chem. A 101 (1997) 831.
[8] M.B. More, D. Ray, P.B. Armentrout, J. Phys. Chem. A 101 (1997) 4254.
[9] M.B. More, D. Ray, P.B. Armentrout, J. Phys. Chem. A 101 (1997) 7007.
[10] M.B. More, D. Ray, P.B. Armentrout, J. Phys. Chem. Soc. 121 (1999) 417.
[11] R.H. Schultz, K.C. Crellin, P.B. Armentrout, J. Am. Chem. Soc. 113 (1991) 8590.
[12] F.A. Khan, D.E. Clemmer, R.H. Schultz, P.B. Armentrout, J. Phys. Chem. 97 (1993) 7978.
[13] N.F. Dalleska, K. Honma, P.B. Armentrout, J. Am. Chem. Soc. 115 (1993) 12125.
[14] N.F. Dalleska, K. Honma, L.S. Sunderlin, P.B. Armentrout, J. Am. Chem. Soc. 116 (1994) 3519.
[15] N.F. Dalleska, B.L. Tjelta, P.B. Armentrout, J. Phys. Chem. 98 (1994) 4191.
[16] M.T. Rodgers, P.B. Armentrout, J. Phys. Chem. A 101 (1997) 1238.
[17] S.E. Hill, E.D. Glendening, D. Feller, J. Phys. Chem. A 101 (1997) 6125.
[18] S.E. Hill, D. Feller, E.D. Glendening, J. Phys. Chem. A 102 (1998) 3813.
[19] E.D. Glendening, D. Feller, M.A. Thompson, J. Am. Chem. Soc. 116 (1994) 10657.
[20] S.E. Hill, D. Feller, unpublished work.
[21] J.W. Grate, R. Strebin, J. Janata, O. Egorov, J. Ruzicka, Anal. Chem. 68 (1996) 333.
[22] See, for example E.P. Horwitz, M.L. Dietz, D.E. Fisher, Solvent Extr. Ion Exch. 9 (1991) 1; E.P. Horwitz, R. Chiarizia, M.L. Dietz, ibid. 10 (1992) 313; R. Chiarizia, E.P. Horwitz, M.L. Dietz, ibid. 10 (1992) 337.
[23] R.H. Schultz, P.B. Armentrout, Int. J. Mass Spectrom. Ion Processes 107 (1991) 29.
[24] D. Gerlich, in State-Selected and State-to-State Ion–Molecule Reaction Dynamics, Part 1. Experiment, C.-Y. Ng, M. Baer (Eds.), Advances in Chemical Physics Vol. 82, Wiley, New York, 1992, pp. 1–176.
[25] K.M. Ervin, P.B. Armentrout, J. Chem. Phys. 83 (1985) 166.
[26] P.B. Armentrout, in Advances in Gas Phase Ion Chemistry, Vol. 1, N.G. Adams, L.M. Babcock (Eds.), JAI, Greenwich, 1992, pp. 83–119.
[27] N. Aristov, P.B. Armentrout, J. Phys. Chem. 90 (1986) 5135.
[28] D.A. Hales, P.B. Armentrout, J. Cluster Science 1 (1990) 127.
[29] D.A. Hales, L. Lian, P.B. Armentrout, Int. J. Mass Spectrom. Ion Processes 102 (1990) 269.
[30] K.A. Holbrook, M.J. Pilling, S.H. Robertson, Unimolecular Reactions, 2nd Ed., Wiley, Chichester, 1996.
[31] S.K. Loh, D.A. Hales, L. Lian, P.B. Armentrout, J. Chem. Phys. 90 (1989) 5466.
[32] M.T. Rodgers, K.M. Ervin, P.B. Armentrout, J. Chem. Phys. 106 (1997) 4499.
[33] S.F. Boys, F. Bernardi, Mol. Phys. 19 (1970) 553.
[34] M. Kaupp, P.v.R. Schleyer, J. Phys. Chem. 96 (1992) 7316.
[35] A.R. Katritzky, N. Malholtra, R. Ramanathan, R.C. Kemerait Jr., J.A. Zimmerman, J.R. Eyler, Rapid Commun. Mass Spectrosc. 6 (1992) 25.
[36] R.M. Izatt, R.E. Terry, B.L. Haynmore, L.D. Hansen, N.K. Dalley, A.G. Avondet, J.J. Christensen, J. Am. Chem. Soc. 98 (1976) 7620.
[37] I. Dzidic, P. Kebarle, J. Phys. Chem. 74 (1970) 1466.
[38] Some values needed for this calculation have not been determined experimentally and are estimated as detailed in [10].
[39] D. Feller, J. Phys. Chem. A 101 (1997) 2723.
[40] B.P. Hay, J.R. Rustad, C. Hostetler, J. Am. Chem. Soc. 115 (1993) 11158.
[41] B.P. Hay, J.R. Rustad, J. Am. Chem. Soc. 116 (1994) 6316.